scientific reports

Check for updates

OPEN

Obesity-induced adipocytes promote diabetes mellitus by regulating β islet cell function through exosome miR-138-5p

Shihong Fan[1] & Nengjuan Li[2]✉

Insulin dysfunction can lead to type 1 diabetes mellitus (T1DM), inducing an increase in blood glucose levels. Unfortunately, there remains a need for more effective clinical treatments for DM. Obesity is closely associated with islet dysfunction, but these inside mechanisms remain unclear. We indicated that obesity-induced adipocytes inhibit insulin secretion (IS) from β islet cells (β-cells) by elevating the expression of their exosome miR-138-5p. Our study proved the high expression of miR-138-5p in exosomes isolated from the fat tissue of obese mice, as well as in exosomes derived from obesity-induced 3T3-L1 cells. The underlying mechanism possibly involves the upregulation of miR-138-5p which suppressed IS while increasing apoptosis in MIN6 cells. miR-138-5p knockdown upregulated insulin production and decreased apoptosis in MIN6 cells. Moreover, dual-luciferase reporter assays revealed the direct regulating effects of miR-138-5p on SOX4. Moreover, SOX4 expression affects the abundance of proteins involved in the Wnt/β-catenin pathway. Under obesity conditions, miR-138-5p in adipocyte exosomes affects IS and ultimately β-cell function by regulating the SOX4-mediated Wnt/β-catenin pathway in β cells. These results not only presented new insights into the interaction between obesity and T1DM but also provide new possible therapeutic mechanisms for obesity-related T1DM.

Keywords Diabetes mellitus, Obesity, Exosome, β islet cell, miR-138-5p, SOX4

Impaired insulin action or insufficient insulin secretion (IS) can lead to diabetes mellitus (DM)[1]. Since insulin is solely produced by pancreatic β-cells (β-cells), the decline in β-cell function accelerates the development of diabetes mellitus (DM)[2]. Glucose is the most effective stimulator for IS. However, dysfunction of β-cells results in defective IS upon glucose stimulation[3].

There is a robust correlation between obesity and islet dysfunction, insulin resistance (IR), and the progression of DM[4–6]. Recent studies have indicated a direct connection of the visceral adiposity index (VAI) with IR among type 2 DM sufferers[7]. Adipocytes are capable of eliciting signals from local sensory nerve fibers for lipolysis and production and transmitting them to distant fat banks or other tissues with metabolic functions to maintain glucose homeostasis[8]. Some studies have mentioned that a high-fat diet can trigger IR and islet cell apoptosis[9], even leading to islet enlargement and hyperinsulinemia[10]. Adipose tissue synthesizes and secretes signaling molecules such as leptin, lipocalin, endoglin, and apelin that affect β-cell function, proliferation, and death[11]. Moreover, it was found that when 3T3-L1 adipocytes were co-cultured with MIN6 cells, IS, and glucokinase expression were significantly reduced[12]. However, the regulatory mechanisms between obesity and islet cell function need to be further explored.

MicroRNAs (miRNAs), typically 19–25 nt in length, are non-coding RNAs. miRNAs can recognize complementary sequences of mRNA sequences and by interfering with mRNA[13], they can be exported to extracellular media via exosomes and proteins, so they can also be found in blood, urine, and cerebrospinal fluid[14–16]. Many miRNAs are involved in the interactions between obesity and islet function. For example, the LNCRNA Tug1/miR-204/SIRT1 axis was experimentally demonstrated to upregulate insulin sensitivity within the adipose tissue of obese mice[17]. miR-23a-3p levels dropped in the fat tissue of the obese and diabetic population[18]. As reported, miR-138-5p can participate in various physiological or disease regulatory processes, such as cancer[19], epilepsy[20], and myocardial injury[21]. Also, it has been proposed that silencing miR-138-5p

[1]Department of Endocrinology, Ningbo Medical Center Lihuili Hospital, Ningbo 315040, Zhejiang, China. [2]Department of Endocrinology, The Second Affiliated Hospital of Zhejiang Chinese Medical University, No. 318 Chaowang Road, Hangzhou 310005, Zhejiang, China. ✉email: linengjuan2007@163.com

boosts glucose uptake in TNF-α-stimulated HepG2 cells[22]. Nevertheless, further investigation is still required to fully elucidate how miR-138-5p influences insulin dysfunction.

miR-138-5p is highly expressed in the exosomes of obesity-induced adipocyte 3T3-L1, which is alleged to regulate β-cell function and apoptosis by inhibiting SOX4 expression in β-cells.

Materials and methods

Animal

The diet-induced obesity (DIO) mouse models (male, 4 weeks of age) utilized in the present study were procured from Cyagen Biosciences, while age- and sex-matched C57BL/6 mice, serving as controls, came from the Laboratory Animal Center of Hangzhou Medical College. The controlled environmental settings were a 12-h light/dark cycle, stable room temperature (RT) at 25 °C, and 50% humidity. Food and water could be freely accessed throughout. After acclimatization lasting one week, experimental procedures were started. We collected adipose tissue from mice after euthanizing them with CO_2. Each animal experiment complied with the protocols approved by the Ethical Committee for Experimental Animal Welfare of the Zhejiang Provincial Laboratory Animal Center (ZJCLA-IACUC-20011121). And the study protocol was conducted in accordance with ARRIVE (Animal Research: Reporting of In Vivo Experiments) guidelines. All methods were performed in accordance with the relevant guidelines and regulations.

Cell culture and induction of obesity

The 3T3-L1 mouse preadipocytes and MIN6 mouse pancreatic β-cells came from the American Type Culture Collection (ATCC, Manassas, USA). Differentiation of 3T3-L1 cells into mature adipocytes was triggered over 7 days using a cocktail containing insulin, 3-isobutyl-1-methylxanthine, dexamethasone, as well as fetal bovine serum (FBS). 300 μmol palmitic acid (0.5 mmol/L) was added to culture mature 3T3-L1 cells for 48 h to simulate obesity-triggered adipocytes. The cells were treated with Dulbecco's modified Eagle medium (DMEM; Gibco, USA) comprising 10% FBS (Gibco, USA) and 100 IU/mL penicillin-streptomycin (PAN-Biotech, Germany) before incubation at 37 °C with 5% CO_2.

Cell transfection

SOX4 overexpression plasmid (OE-SOX4), miR-138-5p inhibitor, miR-138-5p mimic, miR-138-5p antagomir (anti-miR-138-5p), vector, as well as respective negative controls (NC) were constructed at GenePharma (Shanghai, China), and incubated with lipofectamine 2000 reagent (Thermo, USA) after the cell fusion was 80–90%.

Isolation and identification of exosomes

Tissue samples were mechanically minced and subjected to enzymatic digestion for dissociation, followed by filtration for a single-cell suspension. The histiocyte suspension was processed as per a sequential differential centrifugation protocol to isolate exosomes. Initially, the supernatant was centrifuged at 300 ×g for 10 min (4 °C) to remove intact and dead cells. The resulting supernatant was further clarified through centrifugation at 2000 ×g lasting 10 min (4 °C) for cellular debris elimination. Large extracellular vesicles were subsequently pelleted by centrifugation at 10,000 ×g lasting 30 min (4 °C). Finally, the supernatant was ultracentrifuged at 100,000 ×g for 70 min (4 °C) for exosomes. The pellet was washed and resuspended in phosphate-buffered saline (PBS) for downstream applications, yielding the purified exosome fraction.

Exosome morphology was viewed under transmission electron microscopy (TEM; JEOL, Japan). Their particle concentration and size distribution were examined via nanoparticle tracking analysis (NTA), while exosomal marker proteins were detected utilizing Western Blot (WB).

WB

After SDS-PAGE separation, the protein samples were electroblotted onto PVDF membranes (Millipore, USA). After blocking with 5% skim milk for 2 h, the membranes were exposed to primary antibodies (1:1000 dilution) overnight at 4 °C, followed by incubation with HRP-conjugated secondary antibodies (1:5000) for 2 h at RT. The primary antibodies were CD63, CD81, SOX4, Ins1, Ins2, FABP4, Bcl-2, Bax, Caspase-3, β-catenin, and GAPDH (Abcam, USA). Protein signals were identified via an enhanced chemiluminescence (ECL) kit (Beyotime, China). These foregoing antibodies came from Abcam company (USA).

Real-time quantitative PCR (qRT-PCR)

Cell procession was enabled by TRIzol (Thermo, USA) for obtaining total RNA. For miRNA analysis, cDNA synthesis was executed utilizing the TaqMan MicroRNA Reverse Transcription Kit (Applied Biosystems, USA), followed by qRT-PCR enabled by TaqMan Universal Master Mix II (Life Technologies) on an ABI Step-One Plus system (Thermo Fisher Scientific). U6 small nuclear RNA was the internal reference. For mRNA detection, reverse transcription was carried out through PrimeScript™ RT Master Mix (Takara, Japan), and SYBR Premix Ex Taq™ (Takara, Japan) was employed for analysis. GAPDH was the internal reference. The primer sequences were: miR-138-5p-F: AACACGTGAGCTGGTGTTGTGA; miR-138-5p-R: ATCCAGTGCAGGGTCCGAGG; miR-138-5p-RT: GTCGTATCCAGTGCAGGGICCGAGGTATTCGCACTGGATACGACCGGCCT; U6-F: CT CGCTTCGGCAGCACA; U6-R: AACGCTTCACGAATTTGCGT; Ins1-F: GACCATCAGCAAGCAGGTCA; Ins1-R: CAAAAGCCTGGGTGGGTTTG; Ins2-F: AGGACCCACAAGTGGCACAA; Ins2-R: GCTGGTAGAG GGAGCAGATG; GAPDH-F: GGCAAATTCAACGGCACAGTCAAG; GAPDH-R: CGACATACTCAGCACC AGCATCAC.

Enzyme-linked immunosorbent assay (ELISA)
Insulin concentration was quantified via a murine insulin ELISA kit (ExCell Bio, China) as per the manufacturer's guides.

Cell counting Kit-8 (CCK-8) assay
Following 48-h exosome treatment, 20 μL CCK-8 solution was introduced into the culture medium. A 2-h incubation was carried out before measuring the absorbance at 450 nm.

Apoptosis detected by flow cytometry
Cell apoptosis was evaluated through an Annexin V-FITC/PI Apoptosis Detection Kit (40302ES20, Yeasen Biotechnology). Briefly, after preparing the cell suspension, we put 5 μL of Annexin V-FITC and 10 μL of propidium iodide (PI) solution. The samples were incubated in the dark for 10 min. Next, its mixture with 400 μL of binding buffer was gently vortexed. Lastly, apoptotic cells were quantified by flow cytometric analysis.

Oil red O (ORO) staining
Following fixation using 4% paraformaldehyde, the cells were treated with ORO solution for 30 min at RT. Lipid droplets were viewed via a light microscope.

Exosome labeling and Immunofluorescence (IF)
Exosomes were fluorescently labeled with the PKH26 kit (Sigma, USA) as per the manufacturer's protocol. Subsequently, they were gently and slowly resuspended in Diluent C, while in parallel PKH26 dye was added, and the exosomes underwent a 5 min-incubation at RT. After centrifugation lasting 55 min at 100,000 × g, the labeled exosomes were gently gathered. The separated cells were re-dispersed in a medium without serum and maintained with MIN6 cells for 12 h. For nuclear staining, DAPI was added to the culture medium. Fluorescence imaging was executed via a laser scanning confocal microscope (Olympus®, Japan) for labeled exosome observation.

Dual-luciferase assay
To determine the possible binding site of miR-138-5p on SOX4, a bioinformatics prediction analysis was executed via TargetScan. Based on the results of bioinformatics, we chemically synthesized wild-type (wt-SOX4) and mutant (mut-SOX4) sequences. Subsequently, HEK293T cells (SXBIO, China) were transfected with plasmids comprising either the miR-138-5p mimic or an NC. Subsequently, the cells were lysed for 12 min. The suspension was later incubated with luciferase solution (Promega, USA) before measuring the Firefly luciferase intensity. Stop & Glo reagent (Promega, USA) was put into the suspension. The Renilla luciferase intensity was then detected.

Glucose-stimulated IS (GSIS) assay
The culture medium for MIN6 cells was replaced with one without serum for a 24-h culture. The incubation with exosomes lasted 48 h before a 1-h pre-incubation at 37 °C in Krebs-Ringer bicarbonate buffer. Subsequently, MIN6 cells were incubated in Krebs-Ringer bicarbonate HEPES (KRBH) buffer comprising either 2.5 mM or 25 mM glucose for 1 h. IS was quantified via ELISA.

The assay procedure began with the preparation of standard and sample wells, where 50 μL of serially diluted standards or test samples were loaded. Blank wells remained reagent-free. HRP-conjugated detection antibody (100 μL) was introduced into all wells except the blanks. The plate was sealed and incubated (37 °C, 60 min) in a water bath or incubator. The liquid was subsequently aspirated, with the plate gently dried on absorbent paper. Washing involved filling wells with buffer, incubating briefly (1 min), discarding the buffer, and drying five times. 50 μL of each of substrates A and B were piu, followed by a 15-min dark incubation at 37 °C. The reaction was terminated after adding 50 μL of stop solution, and OD450 readings were taken within 15 min.

Statistical analysis
Data were shown in mean ± standard deviation. GraphPad Prism8 enabled the Student's *t*-test to examine the difference. $P < 0.05$ suggests a significant difference. In vivo studies utilized six biological replicates for each experimental group, whereas in vitro assays were conducted with three replicates per group.

Results
miR-138-5p is upregulated in adipose tissue exosomes of DIO mice
Exosomes were successfully isolated from adipose tissue and subsequently characterized. Vesicles exhibiting characteristic exosomal morphology and dimensions were observed using TEM and NTA (Fig. 1A, B). The detection of exosomal markers CD63 and CD81 was verified through WB (Fig. 1C). qRT-PCR results indicated markedly higher miR-138-5p expression in DIO mouse adipose tissue relative to control samples (Fig. 1D). Moreover, miR-138-5p was evidently upregulated in exosomes from the adipose tissue of DIO mice relative to exosomes from control mice.

Induction of adipocytes and construction of cell obesity model in vitro
ORO staining revealed that preadipocytes exhibited a fibroblast-like morphology, characterized by prismatic or polygonal shapes with centrally located nuclei. In contrast, mature adipocytes displayed prominent red lipid droplets within the cytoplasm (Fig. 2A). WB analysis confirmed the fatty acid-binding protein 4 (FABP4) expression in adipocytes, but not in preadipocytes, thereby validating successful adipogenic differentiation (Fig. 2B). To establish an in vitro obesity model, adipocytes were treated with palmitic acid. Subsequent ORO

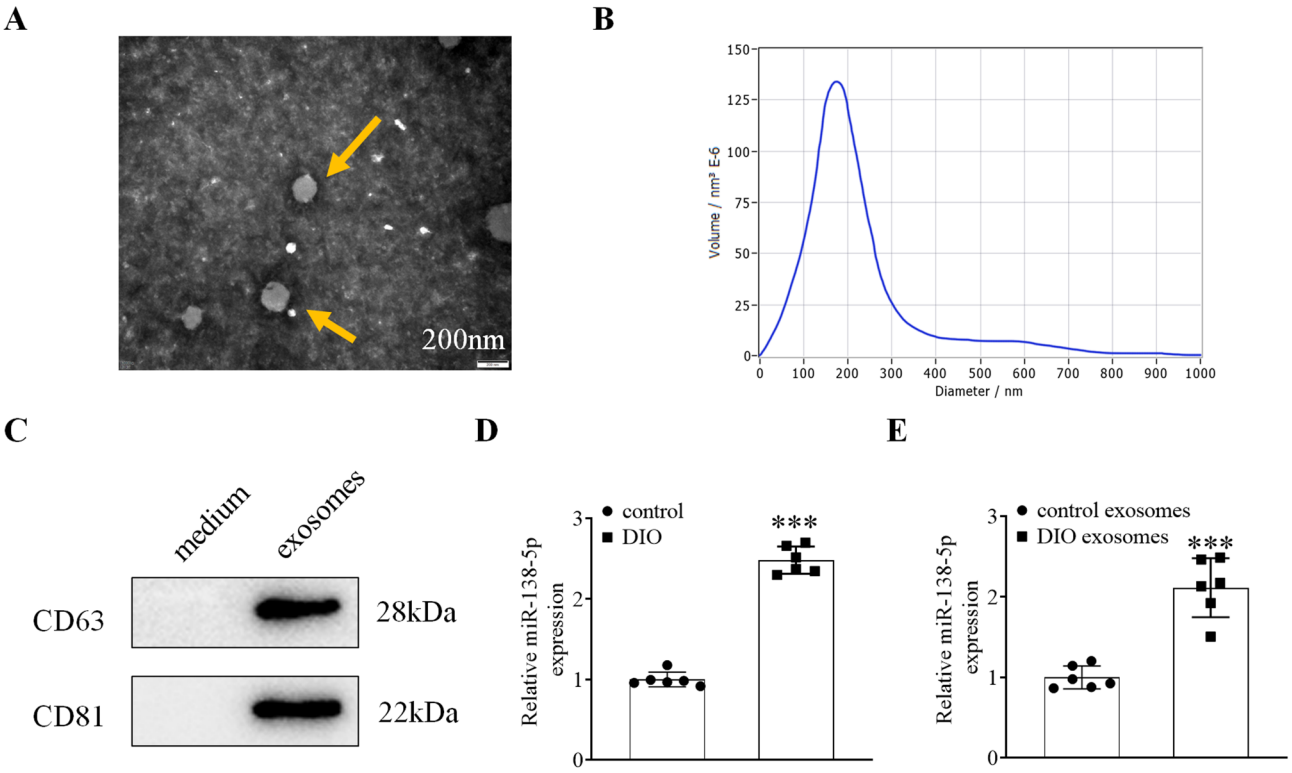

Fig. 1. miR-138-5p is upregulated in adipose tissue exosomes of DIO mice. (**A**) TEM showed that the isolated exosomes exhibited a spherical or ovoid bilayer membrane structure. (**B**) NTA analysis revealed the mean particle diameter of the exosomes of nearly 150 nm. (**C**) WB results indicated positive CD63 and CD81 expression. (**D**) qRT-PCR analysis showed a marked miR-138-5p upregulation in the adipose tissue of DIO mice. (**E**) qRT-PCR analysis demonstrated rising miR-138-5p levels in exosomes derived from adipose tissue of DIO mice. $^{***}P < 0.001$ vs. control cohort.

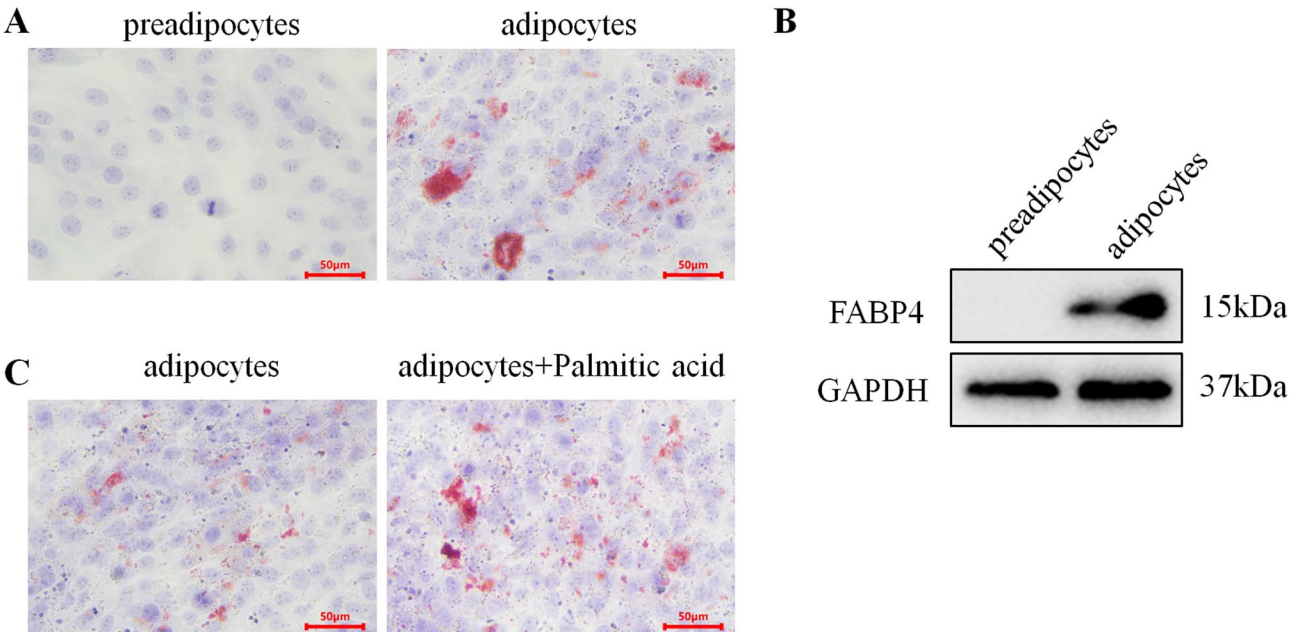

Fig. 2. Induction of adipocytes and construction of cell obesity model in vitro. (**A**) ORO staining demonstrated lipid droplet formation in the adipocytes group. (**B**) FABP4 was positive in the adipocytes group. (**C**) ORO staining indicated that Palmitic acid promoted lipid droplet formation.

staining demonstrated a substantial increase in intracellular lipid droplet accumulation in the palmitic acid-treated adipocytes compared to untreated adipocytes (Fig. 2C). In the following results, the adipocyte group is referred to as the 3T3-L1 group.

miR-138-5p is upregulated in the exosomes of obesity-induced adipocytes

We first collected and identified exosomes from 3T3-L1, which displayed typical morphology and size indicative of exosomes (Fig. 3A, B). Exosomes further showed positive for CD63 and CD81 (Fig. 3C). qRT-PCR experiment revealed a remarkable miR-138-5p upregulation in palmitic acid-induced 3T3-L1 and their exosomes (Fig. 3D, E). Therefore, exosome miR-138-5p is upregulated in obesity-induced adipocytes.

Exosomes of obesity-induced adipocytes cause IS deficiency of β-cells

To investigate whether 3T3-L1 exosomes can be absorbed by MIN6 cells, we labeled the exosomes with PKH26. The results of immunofluorescence staining suggested that the exosomes were absorbed by MIN6 cells (Fig. 4A). We then treated MIN6 cells with exosomes in vitro to assess the inhibitory effect of exosomes from palmitic acid-induced 3T3-L1 cells on the IS capability of β-cells. Results demonstrated that the exosomes inhibited the mRNA expression and content of insulin (Fig. 4B, C). Next, we treated MIN6 cells with glucose and found that the exosomes reduced insulin production (Fig. 4D), decreased the viability of MIN6 cells as well as promoted their apoptosis (Fig. 4E, F, G). Collectively, these results demonstrate that obesity-induced adipocytes inhibit IS and facilitate β-cell apoptosis.

miR-138-5p overexpression in β-cells impairs cell function

To verify whether miR-138-5p affects insulin production, we transferred miR-138-5p mimics into MIN6 cells (Fig. 5A). miR-138-5p mimics highly suppressed insulin mRNA expression levels and content (Fig. 5B, C). We next performed a GSIS experiment on MIN6 cells and discovered that they reduced IS in a high-glucose environment (Fig. 5D). Also, they lowered viability and increased apoptosis of MIN6 cells (Fig. 5E, F, G). This evidence indicates the inhibiting influence of miR-138-5p overexpression on IS and its promoting influence on apoptosis of MIN6 cells.

Knockdown of exosome miR-138-5p alleviates IS deficiency

We further knocked down exosome miR-138-5p in the palmitic acid-induced 3T3-L1 by anti-miR-138-5p (Fig. 6A). miR-138-5p knockdown notably promoted insulin expression (Fig. 6B) while leading to increased

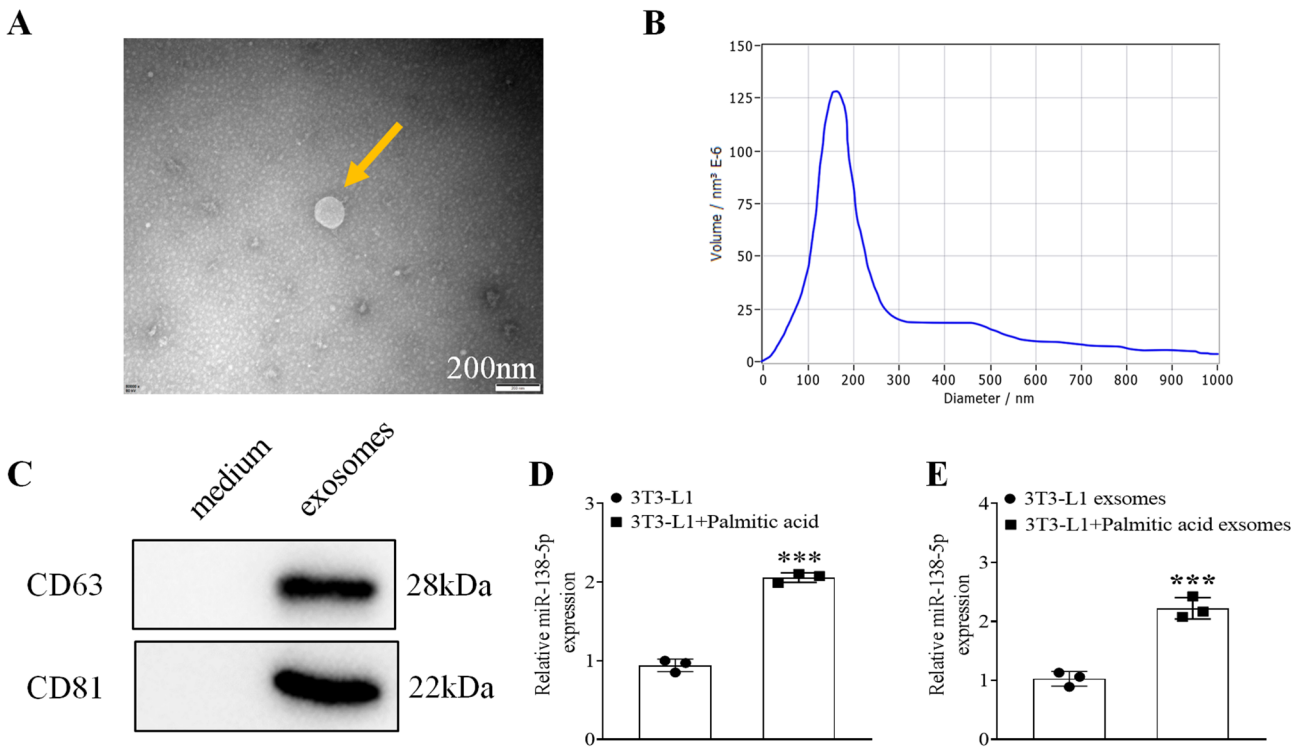

Fig. 3. In vitro identification of exosomes and quantification of miR-138-5p expression. (**A**) Exosomes were observed as spherical or ovoid vesicular structures enclosed by a bilayer membrane. (**B**) NTA analysis revealed the diameter of the exosomes of about 150 nm on average. (**C**) WB results demonstrated positive expression of CD63 and CD81 in the isolated exosomes. (**D**) qRT-PCR indicated upregulated miR-138-5p in the 3T3-L1 cells treated with palmitic acid. (**E**) qRT-PCR showed risen miR-138-5p expression in exosomes from 3T3-L1 cells cultured with palmitic acid. $^{***}P < 0.001$ vs. 3T3-L1 cohort, $^{***}P < 0.001$ vs. 3T3-L1 exosomes cohort.

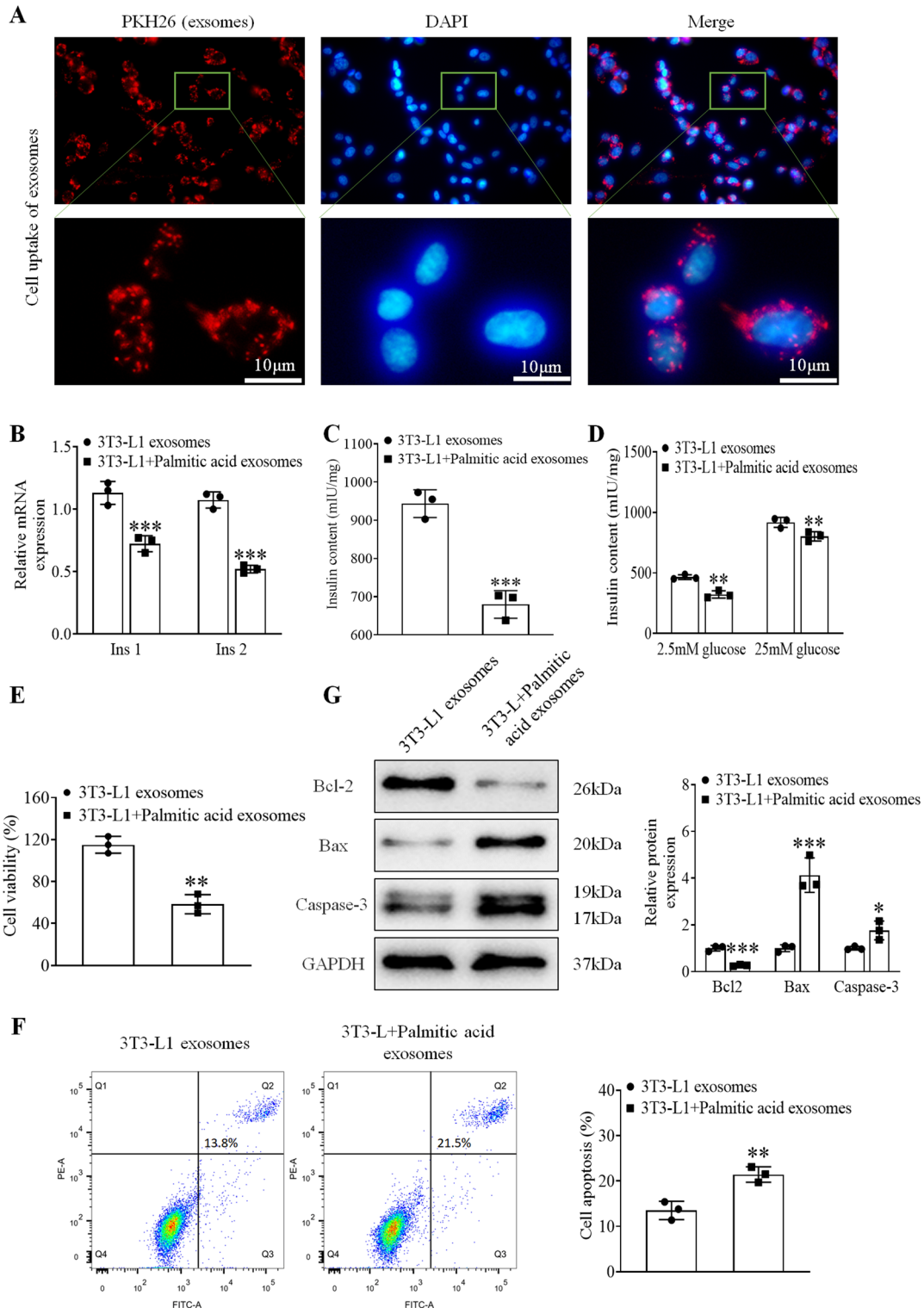

Fig. 4. Exosomes of palmitic acid-induced 3T3-L1 reduced IS and promoted β-cell apoptosis. (**A**) 3T3-L1 exosomes were taken up by MIN6 cells. (**B**) Ins1 and Ins2 were notably lowered in the 3T3-L1 + palmitic acid exosome group. (**C**) The insulin level was significantly reduced in the 3T3-L1 + palmitic acid exosome group. (**D**) The insulin levels were notably decreased in the 3T3-L1 + palmitic acid exosome group. (**E**) Palmitic acid-treated 3T3-L1 cell-derived exosomes reduced MIN6 cell viability. (**F**) Palmitic acid-treated 3T3-L1 cell-derived exosomes induced apoptosis in MIN6 cells. (**G**) WB demonstrated that 3T3-L1 + palmitic acid exosomes promoted apoptosis in MIN6 cells. $^{*}P < 0.05$ vs. 3T3-L1 exosomes cohort, $^{**}P < 0.01$ vs. 3T3-L1 exosomes cohort, $^{***}P < 0.001$ vs. 3T3-L1 exosomes cohort.

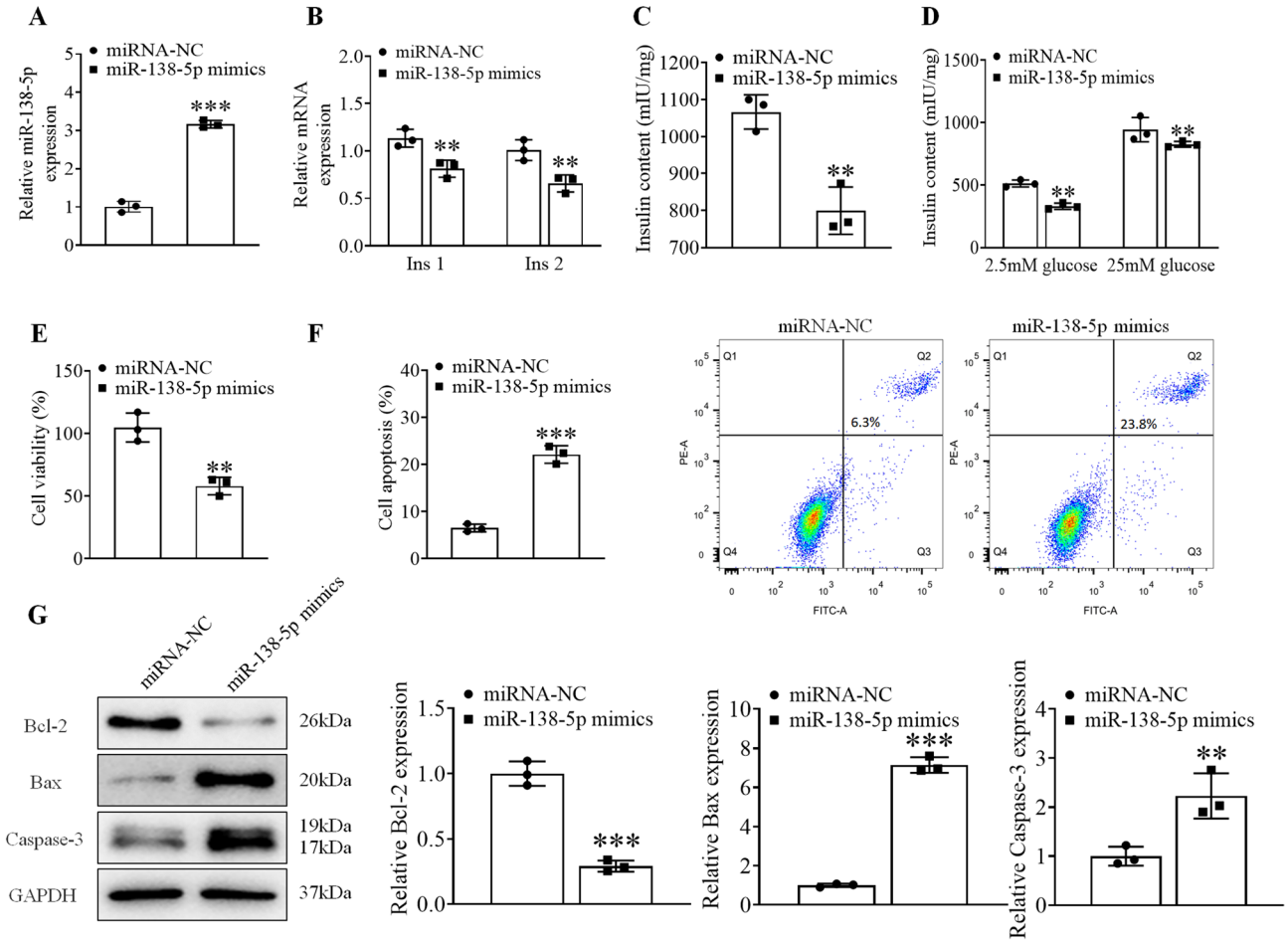

Fig. 5. miR-138-5p overexpression decreased IS and increased apoptosis in MIN6 cells. (**A**) miR-138-5p was upregulated in the miR-138-5p mimics cohort. (**B**) The miR-138-5p mimics cohort demonstrated decreased Ins1 and Ins2. (**C**) The insulin levels dropped in the miR-138-5p mimics group. (**D**) The miR-138-5p mimic cohort exhibited decreased insulin levels. (**E**) miR-138-5p mimics inhibited MIN6 cell activity. (**F**) miR-138-5p mimics promoted MIN6 cell apoptosis. (**G**) WB demonstrated that miR-138-5p mimics increased MIN6 cell apoptosis. $^{**}P<0.01$ vs. miRNA-NC cohort, $^{***}P<0.001$ vs. miRNA-NC cohort.

insulin levels (Fig. 6C). Also, anti-miR-138-5p enhanced the secretion of insulin under high-glucose conditions (Fig. 6D). Anti-miR-138-5p improved cell viability and suppressed apoptosis (Fig. 6E, F, G). In summary, the knockdown of exosome miR-138-5p of palmitic acid-induced 3T3-L1 improves IS and promotes apoptosis in β-cells.

miR-138-5p directly targets SOX4

miR-138-5p target gene prediction was performed through bioinformatics analysis. SOX4 is possible to be a target gene of it (Fig. 7A). miR-138-5p binds directly to the predicted site on SOX4. As anticipated, the combination of wt-SOX4 luciferase reporter and miR-138-5p mimics notably inhibited SOX4-driven luciferase activity in HEK293T cells (Fig. 7B). Furthermore, transfection of the miR-138-5p inhibitor into MIN6 cells effectively downregulated miR-138-5p (Fig. 7C). In contrast, miR-138-5p mimics downregulated SOX4 expressions, whereas miR-138-5p inhibitor upregulated SOX4 expressions (Fig. 7D–E). In summary, miR-138-5p directly targets SOX4.

miR-138-5p reverses the improvement of β-cell function by SOX4-mediated Wnt/β-catenin pathway

We overexpressed SOX4 in MIN6 cells with or without miR-138-5p mimics, and observed that over-expression of miR-138-5p reduced SOX4 expression (Fig. 8A, B). Overexpression of SOX4 did not affect miR-138-5p expression, whereas miR-138-5p mimics significantly enhanced miR-138-5p expression (Fig. 8C). In addition, we observed that elevated SOX4 levels increased β-catenin expression, a key component of the Wnt/β-catenin pathway, whereas miR-138-5p mimics lowered β-catenin levels in OE-SOX4 cells (Fig. 8A, B, C). Upregulation of SOX4 enhanced insulin expression, but the extent was significantly reduced by miR-138-5p mimics (Fig. 8D, E). Under high-glucose conditions, miR-138-5p mimics counteract the effects of elevated IS induced by SOX4 overexpression (Fig. 8F), indicating that miR-138-5p inhibits IS by targeting SOX4. Also, we found that OE-

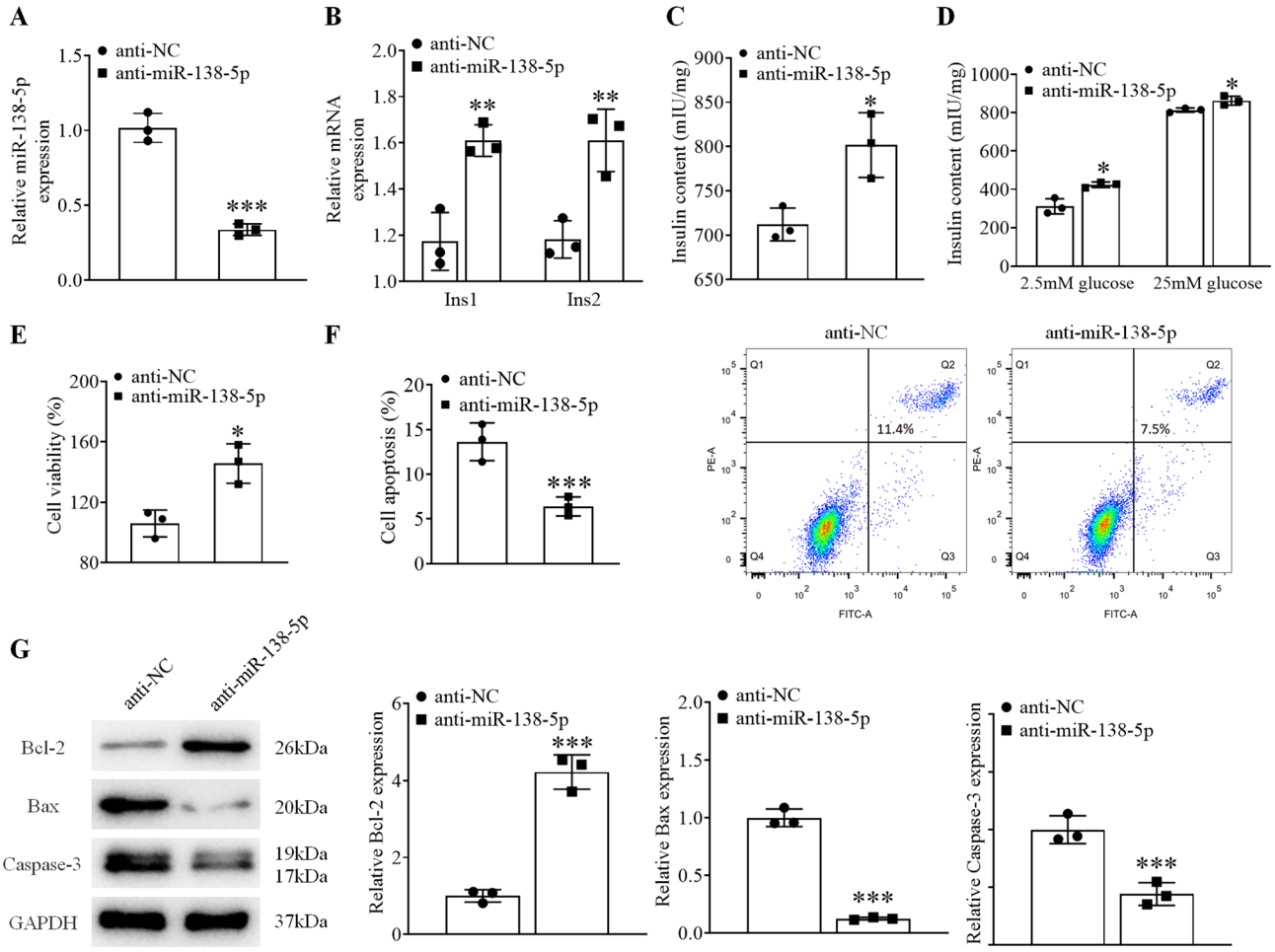

Fig. 6. Knockdown of exosome miR-138-5p improved IS and suppressed MIN6 cell apoptosis. (**A**) The anti-miR-138-5p cohort showed lowered miR-138-5p expression. (**B**) Ins1 and Ins2 levels rose in the anti-miR-138-5p cohort. (**C**) IS was enhanced in the anti-miR-138-5p cohort. (**D**) The anti-miR-138-5p cohort displayed elevated insulin levels. (**E**) Anti-miR-138-5p enhanced MIN6 cell viability. (**F**) MIN6 cell apoptosis was suppressed by anti-miR-138-5p. (**G**) WB proved the inhibiting effects of anti-miR-138-5p on MIN6 cell apoptosis. $^{*}P<0.05$ vs. anti-NC cohort, $^{**}P<0.01$ vs. anti-NC cohort, $^{***}P<0.001$ vs. anti-NC cohort.

SOX4 enhanced cell viability and reduced apoptosis (Fig. 8G, H, I). However, miR-138-5p mimics partially reversed SOX4's effect. Therefore, miR-138-5p influences β cell by targeting the Wnt/β-catenin pathway via SOX4 regulation.

Discussion

Obesity significantly contributes to islet dysfunction and the progression of DM[23,24]. In this study, we found that the exosomes of obese adipocytes may be a mediator of obesity-induced islet dysfunction. Exosomes promote DM by transporting miR-138-5p to β-cells, and miR-138-5p specifically targets SOX4 to suppress IS and facilitate apoptosis in islet cells. These findings demonstrate that adipocyte-derived exosomes can regulate β-cell dysfunction in obesity.

miR-138-5p shows a strong correlation with both adiposity and diabetes. In patients with obesity, human amniotic mesenchymal stem cells exhibit upregulated miR-138-5p[25]. Under high-fat osteogenic stimulation, bone marrow mesenchymal stem cells (BMSCs) showed a 340% higher miR-138-5p expression than their normal counterparts[26]. miR-138-5p has also been noted to have the ability to regulate obesity-associated adipogenesis[27]. It is also extremely critical in regulating islet function. Existing evidence suggests that β islet function and apoptosis regulator (βFaar) can enhance insulin synthesis by selectively adsorbing miR-138-5p, thereby upregulating islet-specific gene Ins2 and NeuroD1; whereas for mice with obesity, βFaar in the islets is significantly downregulated, leading to reduced IS[28]. Nevertheless, how adipose-derived exosomal miR-138-5p influences islet function has not yet been fully investigated. We observed elevated levels of miR-138-5p in the exosomes of adipose tissue, and in both obesity-induced adipocytes and their corresponding exosomes, which caused decreased IS. To further investigate the regulation mechanism between obesity adipocyte-derived exosome miR-138-5p and β-cells, we labeled exosomes with PKH26 and found direct uptake of the exosomes by β-cells. Consequently, exosome miR-138-5p downregulates IS. Besides, upon silencing of exosome miR-138-

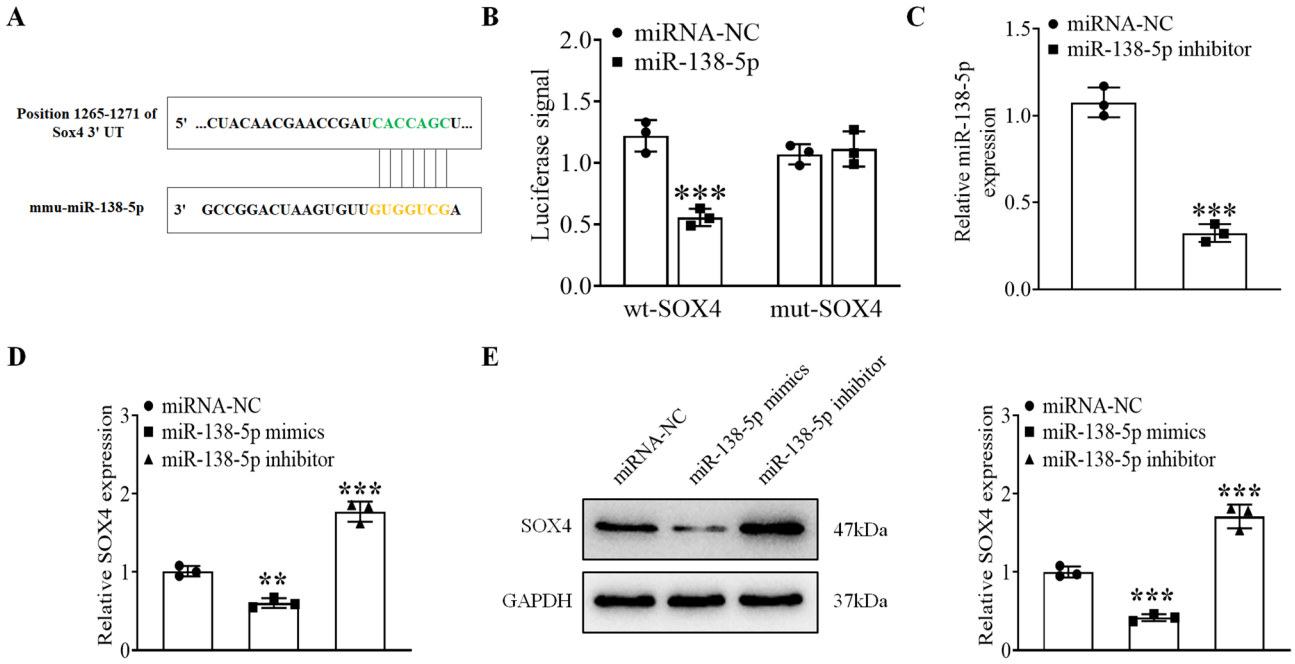

Fig. 7. SOX4 expression is under direct regulation by miR-138-5p. (**A**) Bioinformatics analysis revealed miR-138-5p as a direct regulator of SOX4. (**B**) Luciferase assays confirmed the direct targeting of SOX4 by miR-138-5p. (**C**) Inhibition of miR-138-5p led to its reduced expression. (**D**) SOX4 levels decreased upon miR-138-5p overexpression but rose following miR-138-5p suppression. (**E**) WB showed that the expression of SOX4 was low in the miR-138-5p mimics cohort, and high in the miR-138-5p inhibitor cohort. $^{**}P < 0.01$ vs. miR-NC cohort, $^{***}P < 0.001$ vs. miR-NC cohort.

5p, a notable rise in IS was observed in MIN6 cells. In brief, obesity-induced adipocytes probably regulate the insulin-secreting function of β-cells by the up-regulation of miR-138-5p levels.

Important proteins that regulate IS and release include SOX4, FZD5, CREB1, FOXO1 and GLUT. By regulating the expression of these proteins, miRNAs can impact insulin production and release[29,30]. Among all the proteins in the SOX family, SOX4 exhibits the highest expression level in mouse islets[31]. It has been revealed to be a developmental transcription factor with critical involvement in various biological processes, including proliferation and migration[32–34]. SOX4 was also found to impact the functionality of islets and islet cells[35,36]. Exosome miR-138-5p derived from BMSCs directly targets the 3'UTR region of SOX4 in melanoma cells and miR-138-5p/SOX4 significantly influences cell fate, including cell proliferation and migration[37–39]. However, further investigation is necessitated to clarify if miR-138-5p/SOX4 affects islet dysfunction and elucidate the underlying mechanisms involved.

By conducting this study, we verified the direct regulatory relation of miR-138-5p to SOX4. Inhibition of miR-138-5p significantly boosts impaired cell viability, lowers apoptosis, and enhances proliferation in acute lung injury cellular models[40]. Many miRNAs have been identified to inhibit tumor cell apoptosis by targeting SOX4 [41–43]. For example, the knockdown of SOX4 enhanced apoptosis in breast cancer cells[44]. Our results indicated that OE-SOX4 upregulated the Wnt/β-catenin pathway-related protein β-catenin, promoted the β-cell viability, and inhibited apoptosis, while miR-138-5p mimics reversed these results. The Wnt/β-catenin signaling pathway influences lipid differentiation[45]. Chunbo Li et al. proved that 6-gingerol hinders 3T3-L1 adipocyte differentiation through Wnt/β-catenin activation[46]. Guopan Liu et al. demonstrated that mitochondrial extracellular vesicles can stimulate the TNF-α signaling pathway, activate the Wnt/β-catenin signaling pathway, and dedifferentiate adipocytes[45].

Our study demonstrates the role of adipocytes in transmitting miR-138-5p to β-cells via exosomes in obesity. Moreover, our findings offer novel perspectives on the mechanisms of T1DM development in obese patients, which set a theoretical basis and have practical value for developing novel and improved therapeutic strategies for patients with obesity-related DM.

Conclusion

This study uncovered that obesity-associated adiposity attenuates SOX4 expression in β-cells through the upregulation of miR-138-5p in exosomes. This process subsequently impacts the Wnt/β-catenin signaling pathway, reducing IS and boosting apoptosis in β-cells. In light of the importance of β-cell function and viability in ameliorating T1DM, our findings provide groundbreaking evidence that obesity-induced adipose tissue mediates β-cell dysfunction and apoptosis via miR-138-5p modulation of the SOX4-mediated Wnt/β-catenin pathway. However, further efforts are needed to enhance the clinical relevance of our findings, and our future

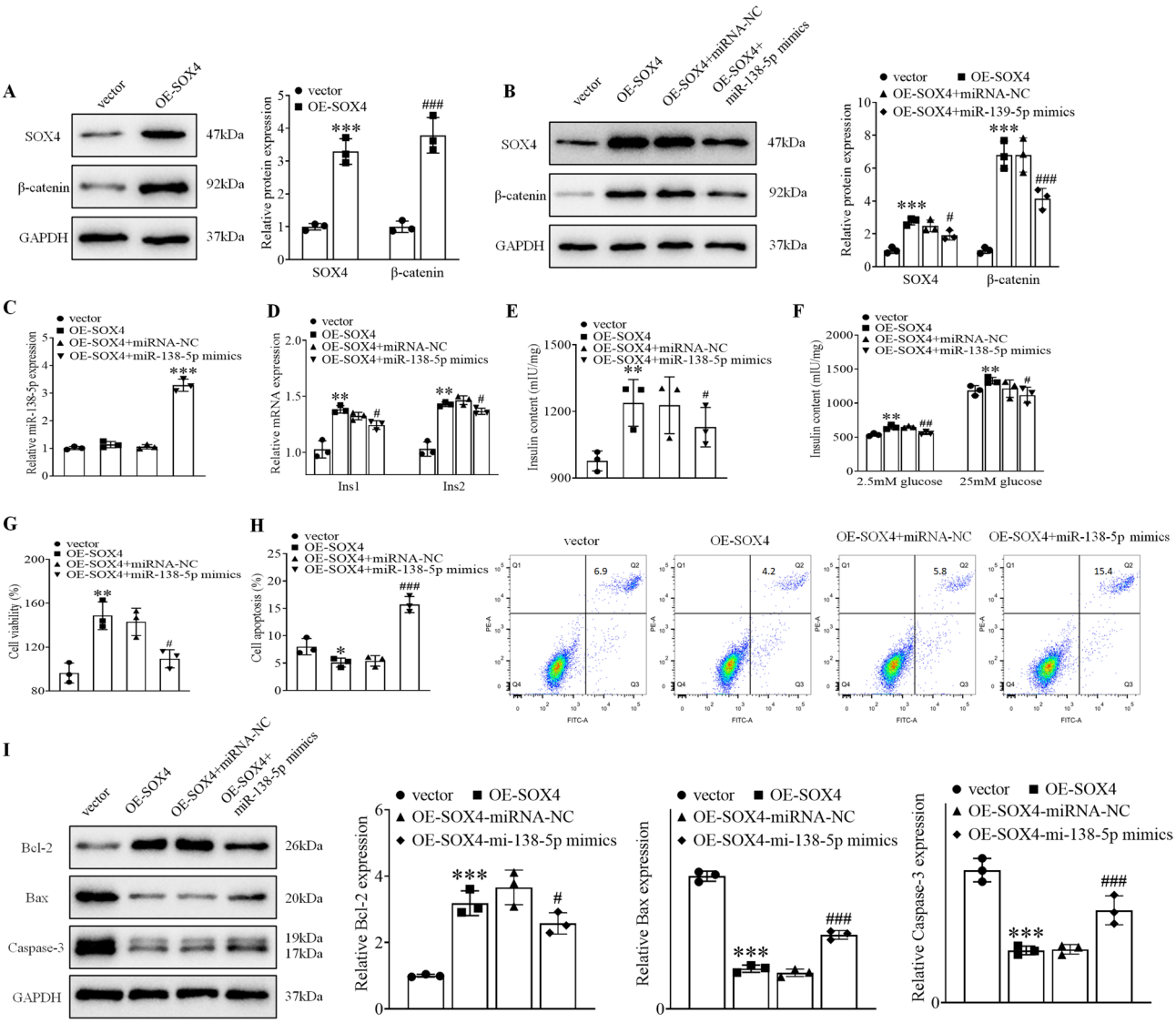

Fig. 8. miR-138-5p overexpression reversed the influence of SOX4 on IS and the apoptosis levels in MIN6 cells. (**A**) WB indicated a marked increase in SOX4 and β-catenin expression in the OE-SOX4 cohort. (**B**) The OE-SOX4 + miR-138-5p mimics group exhibited downregulation of both SOX4 and β-catenin. (**C**) Upregulated miR-138-5p was noted in the SOX4 + miR-138-5p mimics cohort. (**D**) Ins1 and Ins2 levels dropped in the SOX4 + miR-138-5p mimics cohort. (**E**) The insulin level dropped in the SOX4 + miR-138-5p mimics cohort. (**F**) Insulin content was also diminished in the SOX4 + miR-138-5p mimics cohort. (**G**) OE-SOX4 promoted the cellular activity of MIN6 cells, while the SOX4 + miR-138-5p mimics suppressed their activity. (**H**) OE-SOX4 inhibited the apoptosis of MIN6 cells, and SOX4 + miR-138-5p mimics promoted MIN6 cell apoptosis. (**I**) WB showed that OE-SOX4 inhibited MIN6 cell apoptosis, but SOX4 + miR-138-5p mimics promoted it. $^{**}P < 0.01$ vs. vector cohort, $^{***}P < 0.001$ vs. OE-SOX4 + miR-NC cohort, $^{\#}P < 0.05$ vs. OE-SOX4 + miR-NC cohort, $^{\#\#}P < 0.01$ vs. OE-SOX4 + miR-NC cohort, $^{\#\#\#}P < 0.001$ vs. OE-SOX4 + miR-NC cohort.

studies will involve the development of animal models that will provide valuable insights and enable us to investigate the potential applications of our discoveries in a more clinically relevant context.

Data availability

All data to support the conclusions included in this submission.

Received: 30 October 2024; Accepted: 7 May 2025
Published online: 19 May 2025

References

1. Yagihashi, S., Inaba, W. & Mizukami, H. Dynamic pathology of islet endocrine cells in type 2 diabetes: β-Cell growth, death, regeneration and their clinical implications. *J. Diabetes Invest.* **7**, 155–165. https://doi.org/10.1111/jdi.12424 (2016).

2. Janikiewicz, J., Hanzelka, K., Kozinski, K., Kolczynska, K. & Dobrzyn, A. Islet beta-cell failure in type 2 diabetes–Within the network of toxic lipids. *Biochem. Biophys. Res. Commun.* **460**, 491–496. https://doi.org/10.1016/j.bbrc.2015.03.153 (2015).
3. Das, M., Banerjee, A. & Roy, R. A novel in vitro approach to test the effectiveness of fish oil in ameliorating type 1 diabetes. *Mol. Cell. Biochem.* **477**, 2121–2132. https://doi.org/10.1007/s11010-022-04424-1 (2022).
4. Chan, P. C., Liao, M. T., Lu, C. H., Tian, Y. F. & Hsieh, P. S. Targeting Inhibition of CCR5 on improving obesity-associated insulin resistance and impairment of pancreatic insulin secretion in high fat-fed rodent models. *Eur. J. Pharmacol.* **891**, 173703. https://doi.org/10.1016/j.ejphar.2020.173703 (2021).
5. Fernando, S. et al. Metabolic impact of MKP-2 upregulation in obesity promotes insulin resistance and fatty liver disease. *Nutrients* **14** https://doi.org/10.3390/nu14122475 (2022).
6. Barber, T. M., Kyrou, I., Randeva, H. S. & Weickert, M. O. Mechanisms of insulin resistance at the crossroad of obesity with associated metabolic abnormalities and cognitive dysfunction. *Int. J. Mol. Sci.* **22** https://doi.org/10.3390/ijms22020546 (2021).
7. Sung, H. H. et al. The association of the visceral adiposity index with insulin resistance and beta-cell function in Korean adults with and without type 2 diabetes mellitus. *Endocr. J.* **67**, 613–621. https://doi.org/10.1507/endocrj.EJ19-0517 (2020).
8. Guilherme, A., Henriques, F., Bedard, A. H. & Czech, M. P. Molecular pathways linking adipose innervation to insulin action in obesity and diabetes mellitus. *Nat. Rev. Endocrinol.* **15**, 207–225. https://doi.org/10.1038/s41574-019-0165-y (2019).
9. Graus-Nunes, F. et al. Differential effects of angiotensin receptor blockers on pancreatic islet remodelling and glucose homeostasis in diet-induced obese mice. *Mol. Cell. Endocrinol.* **439**, 54–64. https://doi.org/10.1016/j.mce.2016.10.021 (2017).
10. Souza-Mello, V. et al. Comparative effects of Telmisartan, sitagliptin and Metformin alone or in combination on obesity, insulin resistance, and liver and pancreas remodelling in C57BL/6 mice fed on a very high-fat diet. *Clin. Sci. (Lond).* **119**, 239–250. https://doi.org/10.1042/CS20100061 (2010).
11. Dunmore, S. J. & Brown, J. E. The role of adipokines in beta-cell failure of type 2 diabetes. *J. Endocrinol.* **216**, T37–45. https://doi.org/10.1530/JOE-12-0278 (2013).
12. Zhao, Y. F., Feng, D. D., Hernandez, M. & Chen, C. 3T3-L1 adipocytes induce dysfunction of MIN6 insulin-secreting cells via multiple pathways mediated by secretory factors in a co-culture system. *Endocrine* **31**, 52–60. https://doi.org/10.1007/s12020-007-0001-3 (2007).
13. Chen, L. et al. Trends in the development of MiRNA bioinformatics tools. *Brief. Bioinform.* **20**, 1836–1852. https://doi.org/10.1093/bib/bby054 (2019).
14. Estrella Ibarra, P., Garcia-Solis, P., Solis-Sainz, J. C. & Cruz-Hernandez, A. Expression of MiRNA in obesity and insulin resistance: A review. *Endokrynol Pol.* **72**, 73–80. https://doi.org/10.5603/EP.a2021.0002 (2021).
15. Calderari, S., Diawara, M. R., Garaud, A. & Gauguier, D. Biological roles of MicroRNAs in the control of insulin secretion and action. *Physiol. Genom.* **49**, 1–10. https://doi.org/10.1152/physiolgenomics.00079.2016 (2017).
16. Gallo, W., Esguerra, J. L. S., Eliasson, L. & Melander, O. miR-483-5p associates with obesity and insulin resistance and independently associates with new onset diabetes mellitus and cardiovascular disease. *PLoS One.* **13**, e0206974. https://doi.org/10.1371/journal.pone.0206974 (2018).
17. Zhang, Y., Gu, M., Ma, Y. & Peng, Y. LncRNA TUG1 reduces inflammation and enhances insulin sensitivity in white adipose tissue by regulating miR-204/SIRT1 axis in obesity mice. *Mol. Cell. Biochem.* **475**, 171–183. https://doi.org/10.1007/s11010-020-03869-6 (2020).
18. Lozano-Bartolomé, J. et al. Altered expression of miR-181a-5p and miR-23a-3p is associated with obesity and TNFα-Induced insulin resistance. *J. Clin. Endocrinol. Metab.* **103**, 1447–1458. https://doi.org/10.1210/jc.2017-01909 (2018).
19. Zou, Q. T., Lin, Y. & Luo, Q. Y. miR-138-5p inhibits the progression of colorectal cancer via regulating SP1/LGR5 axis. *Cell. Biol. Int.* https://doi.org/10.1002/cbin.11926 (2022).
20. Jin, X. et al. FOXO4 alleviates hippocampal neuronal damage in epileptic mice via the miR-138-5p/ROCK2 axis. *Am. J. Med. Genet. B Neuropsychiatr Genet.* **189**, 271–284. https://doi.org/10.1002/ajmg.b.32904 (2022).
21. Hu, X. et al. CircSAMD4A aggravates H/R-induced cardiomyocyte apoptosis and inflammatory response by sponging miR-138-5p. *J. Cell. Mol. Med.* **26**, 1776–1784. https://doi.org/10.1111/jcmm.16093 (2022).
22. Luan, B. & Sun, C. MiR-138-5p affects insulin resistance to regulate type 2 diabetes progression through inducing autophagy in HepG2 cells by regulating SIRT1. *Nutr. Res. (New York N Y).* **59**, 90–98. https://doi.org/10.1016/j.nutres.2018.05.001 (2018).
23. Tong, Y., Xu, S., Huang, L. & Chen, C. Obesity and insulin resistance: Pathophysiology and treatment. *Drug Discov Today* **27**, 822–830. https://doi.org/10.1016/j.drudis.2021.11.001 (2022).
24. Cheng, X. et al. Long non-coding RNA Meg3 deficiency impairs glucose homeostasis and insulin signaling by inducing cellular senescence of hepatic endothelium in obesity. *Redox Biol.* **40**, 101863. https://doi.org/10.1016/j.redox.2021.101863 (2021).
25. Nardelli, C. et al. miR-138/miR-222 overexpression characterizes the mirnome of amniotic mesenchymal stem cells in obesity. *Stem Cells Dev.* **26**, 4–14. https://doi.org/10.1089/scd.2016.0127 (2017).
26. Wang, F. L. et al. [miR-29c-3p targeted dishevelled 2 on osteogenesis differentiation of rat bone marrow mesenchymal stem cells in high-fat environment]. *Zhonghua Kou Qiang Yi Xue Za Zhi.* **53**, 694–700. https://doi.org/10.3760/cma.j.issn.1002-0098.2018.10.009 (2018).
27. Liu, Y. et al. Circular RNA SAMD4A controls adipogenesis in obesity through the miR-138-5p/EZH2 axis. *Theranostics* **10**, 4705–4719. https://doi.org/10.7150/thno.42417 (2020).
28. Du, Y. et al. Propofol modulates the proliferation, invasion and migration of bladder cancer cells through the miR–145–5p/TOP2A axis. *Mol. Med. Rep.* **23** https://doi.org/10.3892/mmr.2021.12078 (2021).
29. Mysore, R. et al. MicroRNA-221-3p regulates Angiopoietin-Like 8 (ANGPTL8) expression in adipocytes. *J. Clin. Endocrinol. Metab.* **102**, 4001–4012. https://doi.org/10.1210/jc.2017-00453 (2017).
30. Yin, J. et al. MiR-181b suppress glioblastoma multiforme growth through Inhibition of SP1-mediated glucose metabolism. *Cancer Cell Int.* **20** https://doi.org/10.1186/s12935-020-1149-7 (2020).
31. Xu, E. E., Sasaki, S., Speckmann, T., Nian, C. & Lynn, F. C. SOX4 allows facultative β-Cell proliferation through repression of Cdkn1a. *Diabetes* **66**, 2213–2219. https://doi.org/10.2337/db16-1074 (2017).
32. Moreno, C. S. SOX4: the unappreciated oncogene. *Semin Cancer Biol.* **67**, 57–64. https://doi.org/10.1016/j.semcancer.2019.08.027 (2020).
33. Xu, A. L. et al. Circular RNA circ_0011385 promotes cervical cancer progression through competitively binding to miR-149-5p and up-regulating SOX4 expression. *Kaohsiung J. Med. Sci.* **37**, 1058–1068. https://doi.org/10.1002/kjm2.12432 (2021).
34. Geng, H. et al. miR-140 inhibits Porcine fetal fibroblasts proliferation by directly targeting type 1 insulin-like growth factor receptor and indirectly inhibiting type 1 insulin-like growth factor receptor expression via SRY-box 4. *Asian-Australasian J. Anim. Sci.* **33**, 1674–1682. https://doi.org/10.5713/ajas.19.0438 (2020).
35. Schreiber, V. et al. Extensive NEUROG3 occupancy in the human pancreatic endocrine gene regulatory network. *Mol. Metabolism.* **53**, 101313. https://doi.org/10.1016/j.molmet.2021.101313 (2021).
36. Negi, S. et al. Analysis of beta-cell gene expression reveals inflammatory signaling and evidence of dedifferentiation following human islet isolation and culture. *PLoS One* **7**, e30415. https://doi.org/10.1371/journal.pone.0030415 (2012).
37. Lu, Y., Liu, Y., Zhang, K. & Jiang, L. Circular RNA TLK1 exerts oncogenic functions in hepatocellular carcinoma by acting as a CeRNA of miR-138-5p. *J. Oncol.* **2022** (2415836). https://doi.org/10.1155/2022/2415836 (2022).
38. Gao, L. F. et al. Inhibition of MIR4435-2HG on invasion, migration, and EMT of gastric carcinoma cells by mediating MiR-138-5p/Sox4 Axis. *Front. Oncol.* **11**, 661288. https://doi.org/10.3389/fonc.2021.661288 (2021).

39. Wang, X., Cui, Z., Zeng, B., Qiong, Z. & Long, Z. Human mesenchymal stem cell derived exosomes inhibit the survival of human melanoma cells through modulating miR-138-5p/SOX4 pathway. *Cancer Biomark. A*. **34**, 533–543. https://doi.org/10.3233/cbm-210409 (2022).
40. Wu, Y. et al. miR-138-5p targets sirtuin1 to regulate acute lung injury by regulation of the NF-κB signaling pathway. *Can. J. Physiol. Pharmacol.* **98**, 522–530. https://doi.org/10.1139/cjpp-2019-0559 (2020).
41. Li, G., Liu, K., Du, X. & Long Non-Coding RNA TUG1 promotes proliferation and inhibits apoptosis of osteosarcoma cells by sponging miR-132-3p and upregulating SOX4 expression. *Yonsei Med. J.* **59**, 226–235. https://doi.org/10.3349/ymj.2018.59.2.226 (2018).
42. Zhou, W., Cai, C., Lu, J. & Fan, Q. miR-129-2 upregulation induces apoptosis and promotes NSCLC chemosensitivity by targeting SOX4. *Thorac. Cancer*. **13**, 956–964. https://doi.org/10.1111/1759-7714.14336 (2022).
43. Sun, J. C. et al. MiR-499a-5p suppresses apoptosis of human nucleus pulposus cells and degradation of their extracellular matrix by targeting SOX4. *Biomed. Pharmacotherapy = Biomedecine Pharmacotherapie*. **113**, 108652. https://doi.org/10.1016/j.biopha.2019.108652 (2019).
44. Zhang, J., Chai, S. & Ruan, X. SOX4 serves an oncogenic role in the tumourigenesis of human breast adenocarcinoma by promoting cell proliferation, migration and inhibiting apoptosis. *Recent. Pat. Anticancer Drug Discov.* **15**, 49–58. https://doi.org/10.2174/1574892815666200212112119 (2020).
45. Liu, G. et al. Hypertonicity induces mitochondrial extracellular vesicles (MEVs) that activate TNF-alpha and beta-catenin signaling to promote adipocyte dedifferentiation. *Stem Cell. Res. Ther.* **14**, 333. https://doi.org/10.1186/s13287-023-03558-3 (2023).
46. Li, C. & Zhou, L. Inhibitory effect 6-gingerol on adipogenesis through activation of the Wnt/beta-catenin signaling pathway in 3T3-L1 adipocytes. *Toxicol. Vitro* **30**, 394–401. https://doi.org/10.1016/j.tiv.2015.09.023 (2015).

Author contributions

S.F.: Conceptualization, Data curation, Formal analysis, Investigation, Methodology, Visualization, Writing – original draft. N.L.: Methodology, Validation, Project administration, Resources, Supervision.

Funding

This work was supported by the Ningbo Natural Science Foundation (No. 2021J297).

Declarations

Competing interests

The authors declare no competing interests.

Additional information

Supplementary Information The online version contains supplementary material available at https://doi.org/10.1038/s41598-025-01564-4.

Correspondence and requests for materials should be addressed to N.L.